Effect of cementation on the small-strain parameters of sands

A.L. Fernandez and J.C. Santamarina

Abstract: Natural cementation affects the properties of soils, the interpretation of in situ and laboratory test results, and the selection of criteria for geotechnical design. In this paper, published experimental studies are reviewed, a microscale analysis is presented of the effect of cementation on small-strain stiffness for distinct stress–cementation histories, and the effect of cementation on small-strain velocity and damping is experimentally studied. Observations include the prevailing effects of cementation over effective stress, the coexistence of frictional and viscous losses, and the effects of decementation when the medium is unloaded from the level of confinement prevailing during cementation.

Key words: wave velocity, seismic response, stiffness, damping, sampling effects, loading history.

Résumé : La cimentation naturelle affecte les propriétés des sols, l'interprétation des résultats des essais in situ et en laboratoire, et la sélection de critères pour la conception géotechnique. Dans cet article, des études expérimentales publiées sont passées en revue, suivies par une analyse de l'effet de la cimentation sur la rigidité à faible déformation pour les histoires distinctes de cimentation de contraintes. Ensuite, on étudie expérimentalement l'effet de la cimentation sur la vitesse à faible contrainte et sur l'amortissement. Les observations comprennent les effets de la cimentation prévalant sur la contrainte effective, la coexistence des pertes visqueuse en frottement, et les effets de la cimentation lorsque le milieu est déchargé par rapport au niveau de confinement prévalant durant la cimentation.

Mots clés : vitesse d'ondes, réponse sismique, rigidité, amortissement, effets de l'échantillonnage, histoire des contraintes.

[Traduit par la Rédaction]

1. Introduction

Diagenesis begins at the time of soil deposition and continues while the sediment becomes a sedimentary rock. It may involve changes in the surface texture of the material, changes in fabric, the formation of interparticle bonds, and the change in internal distribution of contact forces. Most natural soil deposits possess some degree of cementation resulting from the deposition or precipitation of cementing agent around and at particle contacts. Some of these agents lithify the soil without any modification of the detrital grains. However, other agents produce more complex physicochemical reactions, including changes in the original sediment (Mitchell 1993; Larsen and Chilingar 1979; Blatt 1979).

Cementation, caused by either natural or artificial soil stabilization processes, can have a remarkable influence on the small- and large-strain behavior of soils. Hence, cementation effects should be taken into account in the design of foundations, analysis of the dynamic response of the subsurface, and evaluation of stability problems (see, for example, Arkin and Michaeli 1985; and Poulos 1988).

Received March 3, 1999. Accepted June 1, 2000. Published on the NRC Research Press Web site on February 19, 2001.

A.L. Fernandez and J.C. Santamarina. Civil and Environmental Engineering, Georgia Institute of Technology, Atlanta, GA 30332-0355, U.S.A.

The study of cemented soils in the laboratory demands special specimen preparation and testing procedures. Natural, lightly cemented soils can undergo partial and even complete decementation during sampling. On the other hand, the preparation of artificially cemented specimens in the laboratory can be a challenging task; ideally, artificial specimen preparation and testing should simulate the in situ processes that caused cementation and its history. Two distinct stress–cementation histories can be identified: either the soil stratum is loaded first and cemented afterwards, or the soil is first cemented and then loaded.

This paper reviews published experimental results related to the mechanical behavior of naturally and artificially cemented sands, presents a micromechanical analysis of the small-strain stiffness for different stress–cementation histories, and presents an experimental study on the evolution of small-strain stiffness and damping during cementation and loading. Small-strain parameters do not affect ongoing cementation–decementation processes. Furthermore, the emphasis on small-strain parameters reflects the increased interest for near-surface characterization with seismic waves, and the potential identification of lightly cemented sites with seismic methods.

2. Mechanical properties: prior studies

The small- and large-strain behavior of soils are affected by cementation. A brief review of published data follows.

 DOI: 10.1139/cgj-38-1-191

2.1. Large-strain behavior: peak and residual shear strength

The load–deformation behavior of cemented loose specimens is brittle at low confining pressures and changes towards ductile as confinement increases (Clough et al. 1981; Airey and Fahey 1991; Lade and Overton 1989). Brittle, strain-softening, post-peak behavior is often associated with localization and the formation of fracture planes in cemented soils (Schanz 1998).

The strength of cemented sands depends on the strength of the cementing agent and the strength of sand grains. At low stresses, cementation controls the peak strength, and the shear intercept increases with cement content (Dass et al. 1994; Dupas and Pecker 1979; Acar and El-Tahir 1986). At large stress, the peak angle of shear strength ϕ_{peak} is not significantly changed by the degree of initial cementation (Saxena et al. 1988*a*; Acar and El-Tahir 1986; Reddy and Saxena 1993). After the failure of cementing bonds, the friction between sand grains provides the residual strength, which is characterized by cohesion $c = 0$ and residual angle of shear strength ϕ_{res} independent of the degree of initial cementation.

Cemented specimens are more prone to exhibiting dilative behavior at low confinement, because cemented small particles form highly interlocked large particles (Saxena et al. 1988*b*; Saxena and Lastrico 1978; Lade and Overton 1989). Regions of no breakdown, stable breakdown, and rapid breakdown of cementation have been detected (Airey and Fahey 1991). Typically, such regions correspond to elastic loading without pore-pressure generation, stabilization after pore-pressure buildup, and steady pore-pressure buildup and failure, respectively. Even though cemented sands can liquefy, they possess high initial resistance to volume change which reduces pore-pressure generation and increases their resistance to cyclic liquefaction (Clough et al. 1989).

2.2. Small-strain behavior

Large increments in shear wave velocity due to cementation have been reported in prior studies (for example, Acar and El-Tahir 1986 report a 60% increase); therefore, the natural period of the deposit will be overestimated when uncemented values are used in the analysis. The stiffness increases with cement content. Experimental data by Baig et al. (1997) show that the application of confining stresses to a cemented specimen causes the breakdown of cementation. Hence, overloading cemented specimens can cause a decrease in the maximum shear modulus G_{max}.

Experimental results on the effect of cementation on damping are inconclusive, in part due to differences in load–cementation histories followed during specimen preparation. The following trends are most common among different published results (Chang and Woods 1988; Acar and El-Tahir 1986; Saxena et al. 1988*a*): (*i*) the damping ratio of lightly cemented sands is higher than that corresponding to uncemented sands; and (*ii*) the damping ratio increases as the cement content increases until a peak is reached, then it decreases with further increments in the cement content.

2.3. Summary

The behavior of naturally or artificially cemented sands is affected by cement content, confining pressure, and load–decementation history. Two stress regimes can be identified: a low-stress region where behavior is controlled by the cementation, and a high-stress region where the response is controlled by the state of stress and it resembles the uncemented medium.

3. Micromechanical analysis

The following analysis of the small-strain stiffness of cemented soils is based on the Hertzian contact between two spherical particles. Two cases are considered. In the first case, the load is applied first, then cementation coats the particles. In the second case, the particulate medium is cemented first, and then the load is applied.

3.1. Uncemented particles: Hertzian contact

Consider two elastic spheres of equal radius R subjected to a normal load P. The radius a of the circular contact area is

$$[1] \qquad a = \sqrt{\frac{3(1-\upsilon_m)}{8G_m} PR}$$

where υ_m is Poisson's ratio, and G_m is the shear modulus of the material (Richart et al. 1970; White 1983). The normal load P can be expressed in terms of the average normal stress for an equivalent continuum σ. For a simple cubic packing, the contribution area for one sphere is $4R^2$. Thus

$$[2] \qquad P = 4\sigma R^2$$

The generalization to other packings can be readily implemented, yet the results are little affected. The solution presented herein is clear and simple (for the analysis of random packing, see Chang et al. 1990). Substituting eq. [2] into eq. [1], and dividing by R, the normalized radius of the contact area is

$$[3] \qquad \frac{a}{R} = \sqrt[3]{\frac{3(1-\upsilon_m)}{2} \frac{\sigma}{G_m}}$$

The tangent elastic modulus E_T of the particulate skeleton for uniaxial loading is equal to

$$[4] \qquad E_T = \frac{d\sigma}{d\varepsilon} = \frac{3}{2}\left[\frac{2}{3(1-\upsilon_m)}\right]^{\frac{2}{3}} \left(\frac{\sigma}{G_m}\right)^{\frac{1}{3}} G_m$$

where ε is strain. Rearranging,

$$[5] \qquad E_T = \frac{G_m}{1-\upsilon_m} \sqrt[3]{\frac{3(1-\upsilon_m)}{2} \frac{\sigma}{G_m}}$$

Equation [5] can be written in dimensionless form as

$$[6] \qquad \frac{E_T}{G_m} = \frac{1}{1-\upsilon_m} \sqrt[3]{\frac{3(1-\upsilon_m)}{2} \frac{\sigma}{G_m}} = \frac{1}{1-\upsilon_m} \frac{a}{R}$$

This equation highlights that the normal stiffness of the particulate skeleton at small strain is determined by the size of the contact. This observation can be extended to the computation of stiffness for small-strain perturbations, regardless of the mechanism that produced the contact area (Cascante

Fig. 1. Comparison between the two load–cementation histories: (*a*, *b*) loading before cementation (LbC); (*c*, *d*) cementation before loading (CbL).

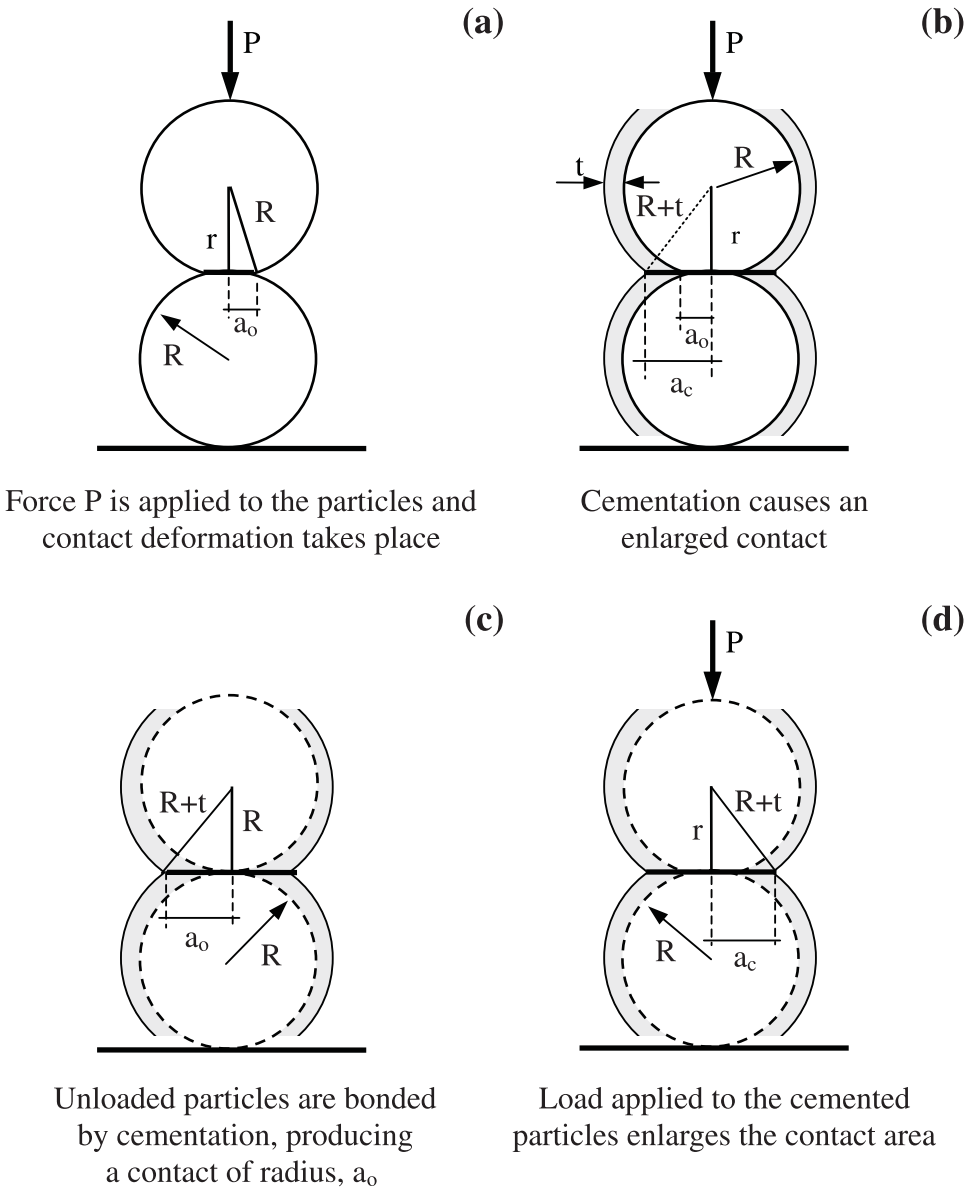

and Santamarina 1996; an alternative approach can be found in George et al. 1985).

3.2. Loading before cementation (LbC)

Loading before cementation is a common sequence in nature, where materials are compressed by the weight of overburden deposits followed by diagenetic cementation processes. The following assumptions are made to model this case: (*i*) after the confinement has been applied, the cementing agent attaches progressively to the surface of spheres, creating a coating of uniform thickness *t*; (*ii*) the cementing material has the same mechanical parameters as the material of the spheres; and (*iii*) compatibility of deformations between the spheres and the cementing agent is satisfied upon further loading, i.e., there is no debonding (applicable until cementation breaks).

These hypotheses are particularly valid in formations such as carbonate sands. The relationship between the cement content by weight, $CC = W_{cement}/W_{particles}$, and the thickness of the coating *t* is readily obtained from geometric considerations (Fig. 1*b*):

$$[7] \qquad 1 + \frac{t}{R} = (CC + 1)^{\frac{1}{3}}$$

This increment in the radius of the spheres has an important effect in the contact area between spheres. The enlarged contact area is a_c:

$$[8] \qquad a_c = a_o + \Delta a$$

where a_o is the contact area produced by the load *P*, as predicted by eq. [1], and Δa is the increment in the radius due to cementation. From Fig. 1, a_c is

$$[9] \qquad a_c = \sqrt{(R+t)^2 - (R^2 - a_o^2)}$$

In dimensionless form

$$[10] \qquad \frac{a_c}{R} = \sqrt{\left(1+\frac{t}{R}\right)^2 - \left[1-\left(\frac{a_o}{R}\right)^2\right]}$$

Combining eqs. [3], [7], and [10],

$$[11] \qquad \frac{a_c}{R} = \sqrt{(CC+1)^{\frac{2}{3}} - 1 + \left[\left(\frac{3(1-\upsilon_m)}{2}\frac{\sigma}{G_m}\right)^{\frac{1}{3}}\right]^2}$$

Substituting eq. [11] in eq. [6] renders the small-strain normal modulus E_T of the cemented skeleton as a function of cementation CC and the applied stress σ:

$$[12] \qquad \frac{E_T}{G_m} = \frac{1}{1-\upsilon_m}\sqrt{(CC+1)^{\frac{2}{3}} - 1 + \left[\left(\frac{3(1-\upsilon_m)}{2}\frac{\sigma}{G_m}\right)^{\frac{1}{3}}\right]^2}$$

3.3. Cementation before loading (CbL)

The second case in the analysis involves a particulate medium that is cemented before the load is applied. This is the most common sequence reproduced in laboratory tests (for example, Saxena et al. 1988*a*; Acar and El-Tahir 1986). Once again, it is assumed that (*i*) the cementing material has the same mechanical parameters as the material of the spheres, and (*ii*) compatibility of deformations between the spheres and the cementing agent is satisfied upon further loading. The initial radius, a_o, of the unstressed but cemented contact is (from geometry)

$$[13] \qquad a_o = [(R+t)^2 - R^2]^{1/2}$$

This would be the radius of the contact produced by a hypothetical confinement σ_{hyp} (from Hertz's theory):

$$[14] \qquad a_o^3 = \frac{3(1-\upsilon_m)}{8G_m}\sigma_{hyp}(2R)^2(R+t)$$

In dimensionless form,

$$[15] \qquad \left(\frac{a_o}{R}\right)^3 = \frac{3(1-\upsilon_m)}{2G_m}\sigma_{hyp}\left(1+\frac{t}{R}\right)$$

Combining eqs. [3], [7], and [15],

$$[16] \qquad \left(\frac{a_o}{R}\right)^2 = \left[\frac{3(1-\upsilon_m)}{2}\frac{\sigma_{hyp}}{G_m}(CC+1)^{\frac{1}{3}}\right]^{\frac{2}{3}} = (CC+1)^{\frac{2}{3}} - 1$$

Thus, the hypothetical stress σ_{hyp} that would produce a similar contact area is

$$[17] \qquad \sigma_{hyp} = \frac{2}{3}\frac{G_m}{1-\upsilon_m}\frac{\left[(CC+1)^{\frac{2}{3}} - 1\right]^{\frac{3}{2}}}{(CC+1)^{\frac{1}{3}}}$$

Fig. 2. Comparison between the two load–cementation histories: micromechanical model (assuming a Poisson's ratio of 0.25).

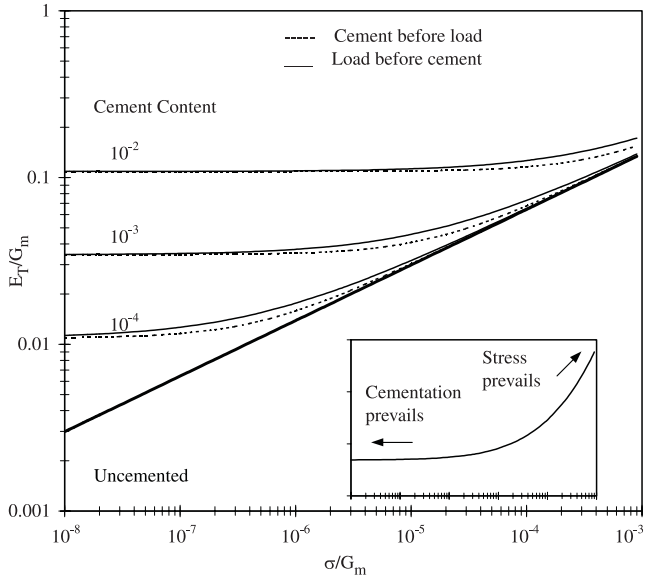

If a stress σ is applied after cementation so that

$$[18] \qquad \sigma' = \sigma_{hyp} + \sigma$$

where σ' is the equivalent stress, the radius of the contact area becomes

$$[19] \qquad \frac{a_c}{R} = \left[\frac{3(1-\upsilon_m)}{2}\frac{\sigma'}{G_m}\right]^{\frac{1}{3}}$$

Then the normal tangent modulus E_T in dimensionless form is

$$[20] \qquad \frac{E_T}{G_m} = \frac{3}{2}\left[\frac{2}{3(1-\upsilon_m)}\right]^{\frac{2}{3}}\left(\frac{\sigma'}{G_m}\right)^{\frac{1}{3}}$$

Combining eqs. [17], [18], and [20],

$$[21] \qquad \frac{E_T}{G_m} = \frac{3}{2}\left[\frac{2}{3(1-\upsilon_m)}\right]^{\frac{2}{3}}\left[\frac{2}{3(1-\upsilon_m)}\frac{\left[(CC+1)^{\frac{2}{3}} - 1\right]^{\frac{3}{2}}}{(CC+1)^{\frac{1}{3}}} + \frac{\sigma}{G_m}\right]^{\frac{1}{3}}$$

3.4. Comparison between the two cases

Equations [12] and [21] capture the interplay between cementation and confinement on the small-strain tangent modulus of a lightly cemented soil. The predicted trends are plotted in Fig. 2. The ratio σ/G_m tends to be very small, hence a small quantity of cement can override the effect of the stress on the small-strain stiffness applicable to many practical geotechnical situations. The normalized modulus E_T/G_m remains constant for small values of the applied stress; this is the "cementation-controlled region." As the applied stress increases, the tangent modulus approaches values

that correspond to the uncemented soil; this is the "stress-controlled region." The existence of these two regions explains conclusions by Poulos (1988) regarding the overprediction of settlement at low confining stress.

For the same cement content and at low confinement, the tangent modulus is greater for the case of loading before cementation than for cementation before loading because particles loaded before being cemented develop a larger contact area (for the same CC). At very low confinements ($\sigma/G_m \rightarrow 0$), the ratio between eqs. [12] and [21], $E_T^{(LbC)}/E_T^{(CbL)}$, approaches 1 + CC/9 (Fig. 2*b*). Results in Fig. 2 clearly show that cementation can be significantly more important than the stress–cementation history of the process (either CbL or LbC).

3.5. Tensile strength decementation

The tensile strength of a cemented specimen is computed assuming that the cement at contacts experiences brittle failure. The tensile strength T of the contact is

$$[22] \quad T = \sigma_T^{cement} \pi a_c^2$$

where σ_T^{cement} is the tensile strength of the cement (an alternative derivation of the tensile strength as a function of the coordination number can be found in Ingles 1962; see also Mitchell 1993). Assuming the area of influence for a particle to be $4R^2$, the tensile strength of the soil is

$$[23] \quad \sigma_T^{soil} = \sigma_T^{cement} \frac{\pi a_c^2}{4R^2}$$

Rearranging terms and invoking eq. [16],

$$[24] \quad \frac{\sigma_T^{soil}}{\sigma_T^{cement}} = \frac{\pi}{4}\left[(CC+1)^{\frac{2}{3}} - 1\right] \approx \frac{\pi}{6} CC$$

The value of σ_T^{soil} is twice the shear intercept in the Mohr-Coulomb space, and it defines the strength of the cemented soil in the cementation-controlled region. This equation also predicts the change in stress a soil can take during unloading before cemented contacts fail, as discussed later in the paper.

4. Experimental study

The experimental study was designed to assess the small-strain variations in stiffness and damping in sands during cementation and stress changes. Two different load–cementation histories were reproduced. Results are also analyzed to elucidate the potential effects of decementation during isotropic loading or unloading.

4.1. Sample preparation

The materials used in these tests are (*i*) fine, subangular, siliceous sand (D_{50} = 0.32 mm, C_c = 0.98, and C_u = 2.1, where C_c and C_u are coefficients of curvature and uniformity, respectively); and (*ii*) Portland cement No. 2, used as cementing agent. The cement content was limited to 2% by weight to produce a lightly cemented specimen. The water to cement ratio was 1.0 to facilitate soil–cement mixing. The water and the cement were mixed first. The sand was added to the paste and specimens were thoroughly mixed for 10 min. The mixture was placed and compacted in layers into a mold inside the resonant column device. The latex membrane was held by vacuum against the wall of the mold (the dry unit weight of specimens was γ = 15.6 kN/m^3; the 7 day unconfined compressive strength was 137.76 kPa and was reached at an axial strain of 1.40%). The complete process of mixing, filling the mold, and assembling the resonant column took less than 45 min. Once the specimen was prepared and the top cap was placed, negative pressure was applied to remove the mold. The negative pressure was eliminated as the desired confining pressure was applied.

Fig. 3. Evolution of small-strain parameters during cementation.

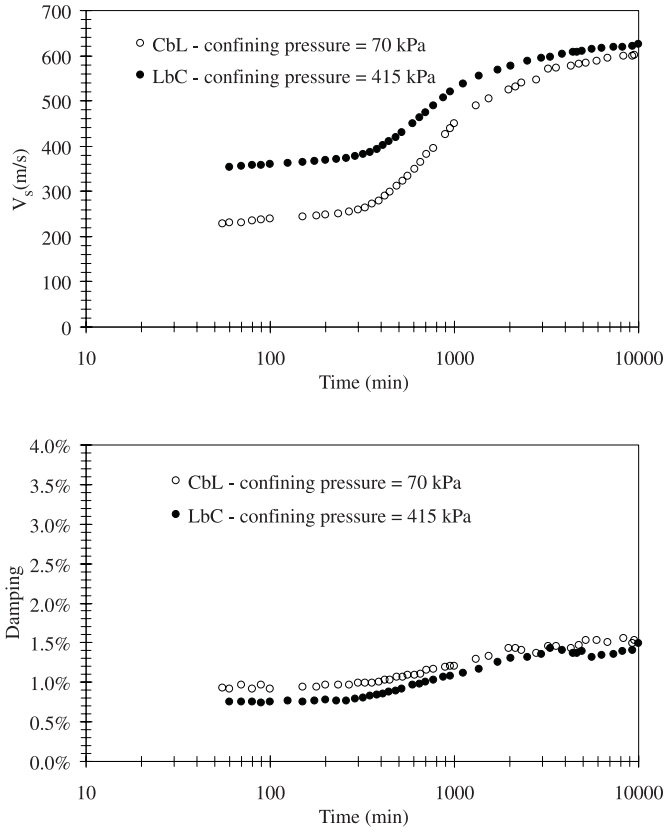

4.2. Resonant column tests

Long-term resonant column tests were run with a Stokoe torsional resonant column device (SBEL D1128). Standard test procedures were modified to excite the column with random noise (Cascante and Santamarina 1997). The shear strain level remained between 1.5×10^{-5} and 5.5×10^{-5} %. The following discussion centers on two complete test sequences (various similar tests were conducted to confirm results in the different regimes and at intermediate conditions).

In the first test, the specimen was left to cure at a confining pressure of 70 kPa. The hardening of the specimen was monitored until its stiffness, in terms of its resonant frequency, became constant (usually 6–7 days). This test sequence simulates cementation before loading (CbL). The confining pressure was then increased to 415 kPa. Finally, the specimen was unloaded to 70 kPa.

The second test simulates a soil subjected to high confining pressure before the cementing agent bonds the particles (LbC). The initial pressure was set to 415 kPa, and the hardening of the material was monitored as in the first test.

Fig. 4. Frequency-dependent damping: viscous and frictional losses.

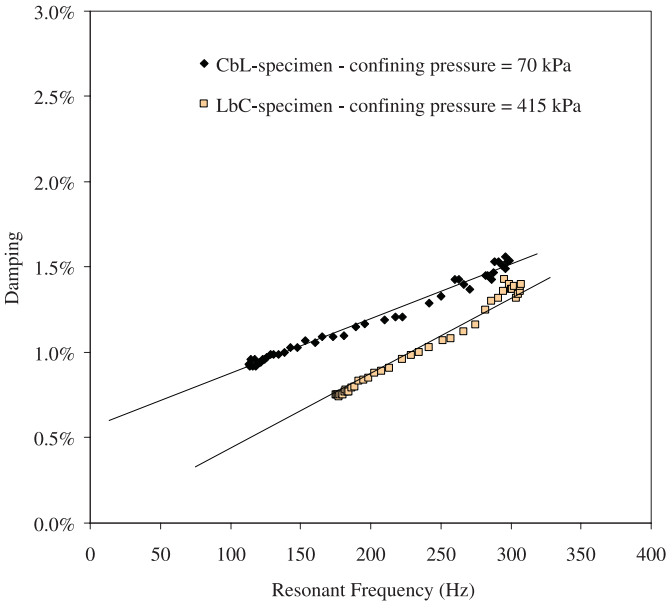

Afterwards, an unload–reload cycle was performed, decreasing the confining pressure to 70 kPa followed by reloading to 415 kPa.

4.3. Experimental results

The time-dependent variations in shear wave velocity and damping during cementation are shown in Fig. 3. For the first 300 min (early hydration stage), there is no influence of the cement on the stiffness of either specimen. The higher stiffness of the LbC specimen reflects the higher applied confinement. As the cement hardens the stiffness of the soil–cement mixtures increases significantly. After 7 days (~10 000 min), the difference in stiffness between the two specimens is small because cementation controls the stiffness in both specimens. At 10 000 min, the ratio of the shear stiffness between the two specimens is about 1.06. The predicted ratio is $E_T^{(LbC)}/E_T^{(CbL)} = 1.02$ (Fig. 2).

The change in damping with time is similar in both tests. Both trends show a slight increase during hardening. The specimen with higher confinement has lower damping, as would be expected in frictional loss. However, damping values D are significantly higher than would be expected for the dry sand skeleton (expected $D \approx 0.5\%$; Santamarina and Cascante 1996). The increase in damping with time cannot be explained from frictional losses, which are expected to decrease with cementation. The effect of frequency as an indicator of viscous losses is explored in Fig. 4 where the measured damping is plotted versus the corresponding resonant frequency (Winkler and Nur 1982; Yale 1985). The linear trend suggests that the measured increment in damping observed in Fig. 3 is of a viscous nature (excess mixing water remains in the specimen). Once stiffness stabilizes (at $t > 3000$ min), the damping ratio remains constant. The overwhelming viscous effects preclude a detailed analysis of the evolution of frictional damping during cementation. Results shown in Fig. 4 are in agreement with experimental data on materials such as sandstones at different moisture contents (e.g., Born 1941). The zero-frequency intercept points to frictional losses (Armstrong 1980; Attewell and Ramana 1966). The higher intercept for the CbL specimen (70 kPa) than for the LbC specimen (415 kPa) supports this hypothesis.

Fig. 5. Change in confinement after cementation, showing the effect on shear wave velocity.

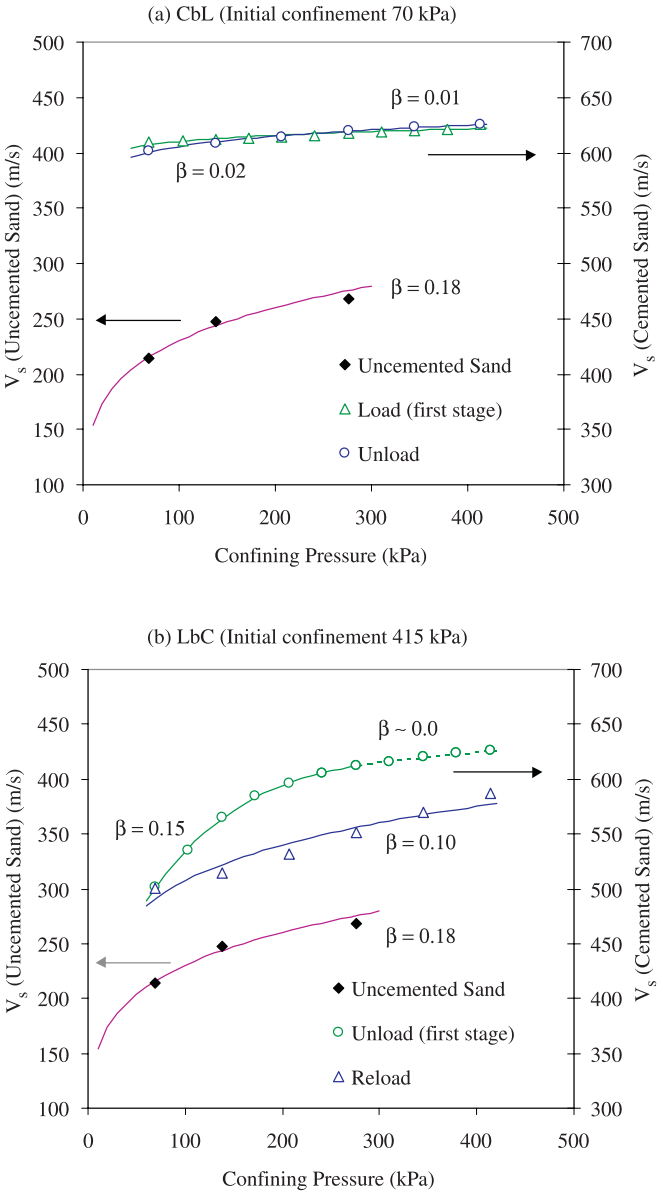

The results for the load–unload cycle for the CbL specimen are shown in Fig. 5*a*. The stiffness of the specimen increases linearly with an increase in the confining pressure. For comparison, velocity–stress data for the uncemented sand are also shown. Results for the unload–reload cycle for the LbC specimen are presented in Fig. 5*b*. In this case, the stiffness of the specimen decreases significantly during unloading, and the loss in stiffness is only partially recovered upon reloading. These results suggest that cemented bonds broke in tension during the initial unloading stage.

Experimental data in Fig. 5 are fitted using the velocity–stress power model $V_s = \alpha\sigma^{\beta}$, where V_s is the shear wave

Fig. 6. Change in confinement after cementation, showing the effect on damping.

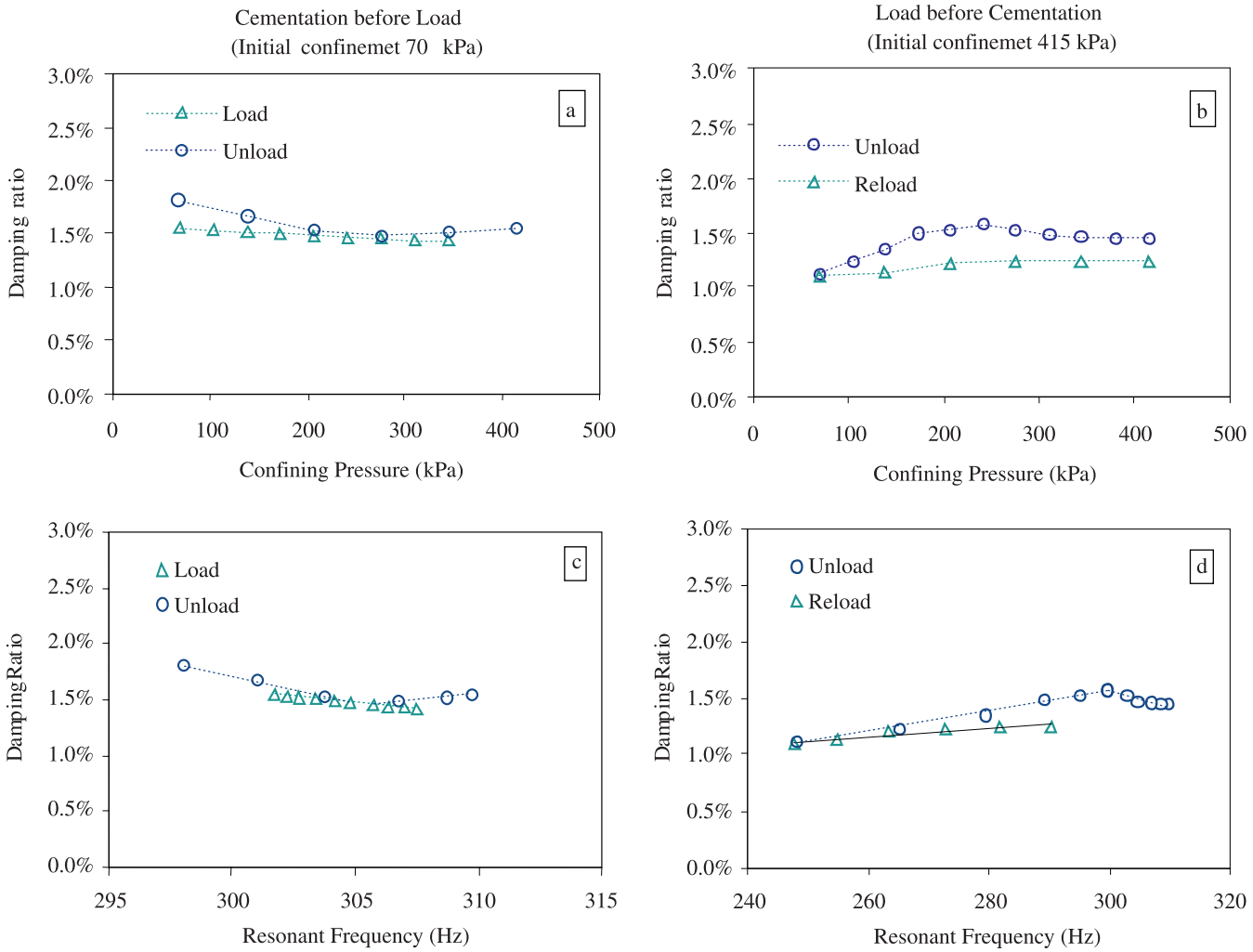

velocity, and α and β are experimentally determined parameters. In the CbL specimen the exponents are very small in both loading and unloading (less than $\beta \approx 0.02$), and the corresponding exponents in the LbC specimen increase to $\beta > 0.1$ The following reference values for the velocity–stress exponent are relevant: $\beta = 0.25$ for uncemented sands, $\beta = 0.17$ for particulate media with Hertzian contact, and $\beta = 0$ for linear solids (see a related discussion in Aloufi and Santamarina 1995). These results show that light cementation is sufficient to mask the particulate, nonlinear nature of the soil at small strains.

The clear difference in the evolution of stiffness between the two specimens shows that unloading is more detrimental to the cemented material than isotropic loading. Furthermore, a medium cemented after loading experiences tension in the cementation bridges during unloading, leading to decementation (loaded particles act like compressed springs; if cementation develops after loading, particles stretch during unloading and the cement goes into tension).

The evolution of damping during the load cycle is plotted in Fig. 6. Damping decreases with increasing confining pressure in the CbL specimen, and both loading and unloading paths are similar (Fig. 6*a*). In the LbC specimen, the damping increases as the confinement pressure decreases, following the same behavior as that of the first specimen until cemented bonds start breaking (~240 kPa, which corresponds to ~175 kPa of unloading; refer to eq. [24]); therefore damping decreases as the sample is unloaded (Fig. 6*b*). It is difficult to separate viscous from frictional contributions in these plots. Figures 6*c* and 6*d* present the same damping data plotted against frequency. The region where damping decreases with increasing confinement and increasing frequency reflects prevailing frictional losses.

4.4. Additional observations

Experimental results from both CbL and LbC tests have been used to validate the micromechanical models of cementation, for a cement content CC = 0.5% (Fig. 7). The CbL model is compared with the loading stage of the CbL experiment. As for the LbC model, the experimental data shown correspond to the first part of the unloading stage, before decementation occurs. The fitting parameters used in modeling the data are the shear wave velocity in the cementing material (V_{sm} = 3500 m/s) and Poisson's ratio (υ_m = 0.20).

The increase in damping during cementation was explained as the effect of viscous damping associated with the increase in resonant frequency. However, an alternative hypothesis may be raised related to limitations in resonant

Fig. 7. Comparison between experimental data and predictions based on the micromechanical models (fitting parameters: V_{sm} = 3500 m/s and υ_m = 0.20).

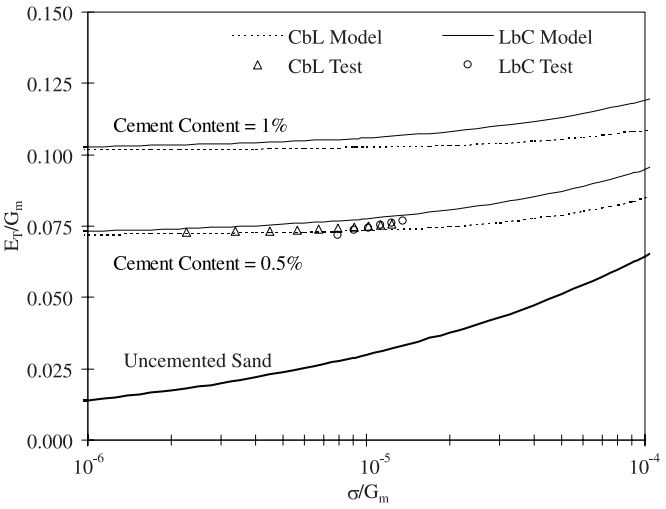

column testing: as the specimen becomes stiffer, the impedance mismatch between the specimen and the bottom plate of the resonant column device decreases, and energy may leak through the base. This hypothesis was tested with calibration specimens of different resonant frequencies (within the range of the tests). The device was clamped at the base to various masses. Similar damping values were obtained in all cases. Therefore, it is concluded that trends observed in Fig. 3*b* reflect viscous damping effects only.

5. Conclusions

Published data and new experimental results obtained in this study support the following observations:

(1) The effect of cementation on strength and stiffness prevails at low stress. At high stress, the particulate nature of the medium takes over, rendering stress-dependent strength and stiffness. The transition stress between the low- and high-stress regimes increases with the amount of cementation.

(2) In the low-stress "cementation-controlled region," soils exhibit brittle behavior, even in fairly loose specimens, and localization is expected. Dilation tends to be higher for cemented sands than for uncemented sands.

(3) Changes in isotropic confinement can cause decementation. The effect is more pronounced when the medium is unloaded from the level of confinement prevailing during cementation, because cementation bonds are subjected to tension. In this context, the load–cementation history is important.

(4) The small-strain stiffness of sands can increase by an order of magnitude or more due to cementation.

(5) Load before cementation produces a medium with higher stiffness than cementation before loading, but the difference is relatively small. In this case, the load–cementation history is not relevant.

(6) Cemented soils exhibit very limited changes in wave velocity due to stress changes, until decementation begins to take place. Hence, small cementation can hide the particulate nature of soils as manifested at small strains.

(7) Changes in damping during cementation must be carefully analyzed. In particular, comparisons must be made at the same frequency and moisture, due to the prevailing effect of viscous damping.

Acknowledgements

Support for this research was provided by Petroleos de Venezuela PDVSA-INTEVEP and the National Science Foundation. The authors are grateful to the reviewers for valuable comments and suggestions.

References

Acar, Y., and El-Tahir, A. 1986. Low strain dynamic properties of artificially cemented sand. Journal of Geotechnical Engineering, ASCE, **112**(11): 1001–1015.

Airey, D.W., and Fahey, M. 1991. Cyclic response of calcareous soil from the north-west shelf of Australia. Géotechnique, **41**(1): 101–121.

Aloufi, M., and Santamarina, J.C. 1995. Low and high strain mechanical properties of grain masses — the effect of particle eccentricity. Transactions of the American Association of Agricultural Engineers, **38**(3): 877–887.

Arkin, Y., and Michaeli, L. 1985. Short- and long-term erosional processes affecting the stability of the Mediterranean coastal cliffs of Israel. Engineering Geology, **21**: 153–174.

Armstrong, B. 1980. Frequency-independent background internal friction in heterogeneous solids. Geophysics, **45**(6): 1042–1054.

Attewell, P.B., and Ramana, Y.V. 1966. Wave attenuation and internal friction as functions of frequency in rocks. Geophysics, **31**(6): 1049–1056.

Baig, S., Picornell, M., and Nazarian, S. 1997. Low strain shear moduli of cemented sands. Journal of Geotechnical Engineering, ASCE, **123**(6): 540–545.

Blatt, H. 1979. Diagenetic processes in sandstones. Society of Economic Paleontologists and Mineralogists, Special Publication 26, pp. 141–157.

Born, W.T. 1941. The attenuation constant of earth materials. Geophysics, **6**(2): 132–148.

Cascante, G., and Santamarina, J.C. 1996. Interparticle contact behavior and wave propagation. Journal of Geotechnical Engineering, ASCE, **122**(10): 831–839.

Cascante, G., and Santamarina, J.C. 1997. Low-strain measurements using random noise excitation. Geotechnical Testing Journal, **20**(1): 29–39.

Chang, T.S., and Woods, R.D. 1988. Internal damping of composite cementitious material: cemented sand. *In* Recent Advances in Ground-Motion Evaluation, Proceedings of the 2nd Conference of Earthquake Engineering and Soil Dynamics. ASCE Geotechnical Special Publication, New York, pp. 359–373.

Chang, C.S., Misra, A., and Sundaram, S.S. 1990. Micromechanical modeling of cemented sands under low amplitude oscillations. Géotechnique, **40**(2): 251–263.

Clough, G.W., Sitar, N., Bachus, R.C., and Rad, N.S. 1981. Cemented sands under static loading. Journal of Geotechnical Engineering, ASCE, **107**(6): 799–817.

Clough, G.W., Iwabuchi, J., Rad, N.S., and Kuppusamy, T. 1989. Influence of cementation on the liquefaction of sands. Journal of Geotechnical Engineering, ASCE, **115**(8): 1102–1117.

Dass, R.N., Yen, S.C., Das, B.M., Puri, V.K., and Wright, M.A. 1994. Tensile stress–strain characteristics of lightly cemented sand. Geotechnical Testing Journal, **17**(3): 305–314.

Dupas, J.M., and Pecker, A. 1979. Static and dynamic properties of sand-cement. Journal of the Geotechnical Engineering Division, ASCE, **105**(GT3): 419–435.

George, T.L., Kennedy, T.C., and Peddicord, K.L. 1985. An elastic stress–strain relation for sphere arrays undergoing initial stage sintering. Transactions of the American Society of Mechanical Engineers, **52**: 98–104.

Ingles, O.G. 1962. Bonding forces in soils. Part 3: a theory of tensile strength for stabilized and naturally coherent soils. *In* Proceedings of the 1st Conference of the Australian Road Research Board, Vol. 1, pp. 1025–1047.

Lade, P.V., and Overton, D.D. 1989. Cementation effects in frictional materials. Journal of Geotechnical Engineering, ASCE, **115**: 1373–1387.

Larsen, G., and Chilingar, G.V. 1979. Diagenesis in sediments and sedimentary rocks. Elsevier Scientific Publishing Company, New York.

Mitchell, J.K. 1993. Fundamentals of soil behavior. 2nd ed. John Wiley and Sons, Inc., New York.

Poulos, H.G. 1988. The mechanics of calcareous sediments. John Jaeger Memorial Address, Australian Geomechanics, Australian Geotechnical Society, Special Edition.

Reddy, K.R., and Saxena, S.K. 1993. Effects of cementation on stress–strain and strength characteristics of sands. Soils and Foundations, **33**(4): 121–134.

Richart, F.E., Hall, J.R., and Woods, R.D. 1970. Vibrations of soils and foundations. Prentice-Hall, Inc., Englewood Cliffs, N.J.

Santamarina, J.C., and Cascante, G. 1996. Stress anisotropy and wave propagation: a micromechanical view. Canadian Geotechnical Journal, **33**: 770–782.

Saxena, S.K., and Lastrico, R.M. 1978. Static properties of lightly cemented sands. Journal of the Geotechnical Engineering Division, ASCE, **104**(12): 1449–1464.

Saxena, S.K., Avramidis, A.S., and Reddy, K.A. 1988*a*. Dynamic Moduli and damping ratios for cemented sands at low strains. Canadian Geotechnical Journal, **25**: 353–368.

Saxena, S.K., Reddy, K.R., and Avramidis, A.S. 1988*b*. Static behavior of artificially cemented sands. Indian Geotechnical Journal, **18**(2): 111–141.

Schanz, T. 1998. A constitutive model for cemented sands. *In* Localization and bifurcation theory for soils and rocks. *Edited by* T. Adachi, F. Oka, and A. Yashima. A.A. Balkema, Rotterdam, The Netherlands, pp. 165–172.

White, J.E. 1983. Underground sound. Application of seismic waves. Elsevier Science Publishers B.V., Amsterdam, The Netherlands.

Winkler, K.W., and Nur, A. 1982. Seismic attenuation: effects of pore fluids and frictional sliding. Geophysics, **47**(1): 1–15.

Yale, D. 1985. Recent advances in rock physics. Geophysics, **50**(12): 2480–2491.